21st Australasian Fluid Mechanics Conference
Adelaide, Australia
10-13 December 2018

A Numerical Investigation into the Effects of Inclination on the Development of Slugging in Channel Flow

J. A. Giddings[1] **and J. Billingham**[2]

[1]Department of Applied Mathematics
The University of Adelaide, South Australia 5005, Australia

[2]School of Mathematical Sciences
The University of Nottingham, Nottingham, NG7 2RD, UK

Abstract

Gas-liquid pipe flows are extremely important in many industries, one of which is the oil/gas industry which is where the motivation for this work comes from and where the transition to a slug flow regime is undesirable. It has been shown that, for constant inclination, two steady-state solutions exist which result in a saddle-node bifurcation and means that there are no uniform steady state solutions for sufficiently uphill flow [5]. We will provide a brief overview of the model — a hydraulic model for turbulent, two-layer, gas–liquid flow with gas velocity much greater than liquid velocity, in a horizontal channel — and steady-state analysis covered by Giddings & Billingham [5] before extending their numerical investigation into the effects of inclination on the development of slugging. This leads to the discovery that an uphill section followed by a horizontal section produces larger roll waves in the horizontal section than would otherwise be formed. This is of particular importance as subsea natural gas pipelines must travel uphill as they leave the sea before travelling across land which may result in larger roll waves, and potentially slugs, forming. Further, we will demonstrate, numerically, the likely formation of a slug at any point where the angle of inclination of the channel is anywhere equal to that of the saddle-node bifurcation angle.

Introduction

In subsea natural gas pipelines the gas is compressed before being pumped through the pipe at high pressure, resulting in a highly turbulent flow. As it flows through the pipe some of the gas condenses into a low density liquid. When gas and liquid flow together there are several possible flow regimes that can occur depending on the velocity of the gas and liquid — the main types we are interested in are stratified flow and slug flow. The study of the formation of slug flow regimes in two-layer hydraulic flow has mainly been aimed at investigating the point at which a stratified flow becomes unstable via linear stability theory, better known as the Kelvin-Helmholtz instability [3, 10, 15]. However, in order to understand the transition to slug flow we must take into account the non-linear effects [11]. When a multiphase flow is above the Kelvin-Helmholtz instability limit, small disturbances will grow and form into roll waves [1] which may annihilate each other forming larger roll waves in an open channel [8], this may result in a transition into a slug flow regime in a closed channel.

Subsea natural gas pipelines lie on the seabed and follow the topography of the sea floor. This may destabilise the flow. Further, as the pipeline comes to shore it will be at a slight incline before reaching a processing plant, so the effects of uphill inclination are of particular importance. Linear stability analysis of the shallow-water equations over uneven surfaces shows that low-amplitude topography destabilises the flow and allows roll waves to form for lower Froude numbers, whilst higher-amplitude topography has a stabilising effect on the flow [2], consistent with observations of hydraulic engineers [12, 14].

Giddings & Billingham [5] extended the model of Needham *et al.* [13] — a hydraulic model for turbulent, two-layer, gas–liquid flow with gas velocity much greater than liquid velocity, in a horizontal channel — to include the effect of a small, spatially-varying inclination. In this paper, we provide a brief overview of their work before expanding on their numerical investigation into the effects of a varying angle of inclination on the development of a slug flow regime.

We are specifically concerned with two phase flow at high pressure, where the density of the overlying gas is very significant. In Johnson *et al.* [7], experiments using sulphur hexaflouride, which is dense enough that it mimics the effect of the extreme pressures that exist in subsea pipelines, show that roll waves that match well with a model similar to the one that we use here, are seen to form on the free surface. 3D effects can of course sometimes be important, but our model is designed for the roll wave regime, and specifically to investigate the effect of inclination on the flow and its role in slug formation. Since we have studied flow in a channel, we should not expect to be able to compare directly with pipeline experiments, but we would expect that our broad qualitative observations on the effect of changes in channel inclination on the dynamics of roll waves and the development of slugs would be correct.

The Hydraulic Model

We study long wavelength, two-layer, turbulent channel flow of gas over liquid at an angle $\theta(x)$ with the horizontal. We find that, in the thin film limit (i.e. the effects of the channel top are neglected), for dimensionless height of the fluid layer, h, fluid layer velocity, v, and slope of the channel, $\bar{\theta} = \theta/c_l$ where c_l is a (small) Chézy coefficient, the governing equations are given by

$$h_t + [hv]_x = 0, \tag{1}$$

$$v_t + vv_x + \frac{1-\rho}{F_0^2}\left(h_x + \bar{\theta}\right) = -\frac{v|v|}{h} + \frac{h+\lambda}{(1+\lambda)h} + \frac{1}{hR_l}\left[hv_x\right]_x, \tag{2}$$

subject to the unique steady state in the horizontal channel, $h = 1$, $v = 1$ when $\bar{\theta} = 0$. Here R_l is the effective Reynolds number in the fluid layer, whilst the density ratio, Froude number and drag parameter are defined to be

$$\rho = \frac{\rho_g}{\rho_l}, \quad F_0 = \frac{q_l}{\sqrt{gh_0^3}}, \quad \lambda = \frac{c_l^g}{c_g}\frac{A}{h_0}, \tag{3}$$

for (constant) densities of the gas and liquid phases, ρ_g and ρ_l, fluid volumetric flowrate, q_l, equilibrium fluid layer depth, h_0, acceleration due to gravity, g, channel height, A, and Chézy coefficients, c_g and c_l^g. For the full derivation and discussion of the parameters see [4].

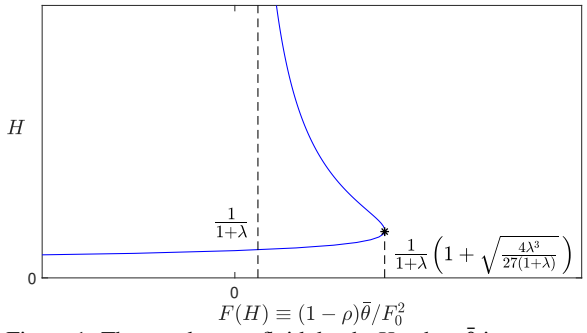

Figure 1: The steady state fluid depth, H, when $\bar{\theta}$ is constant.

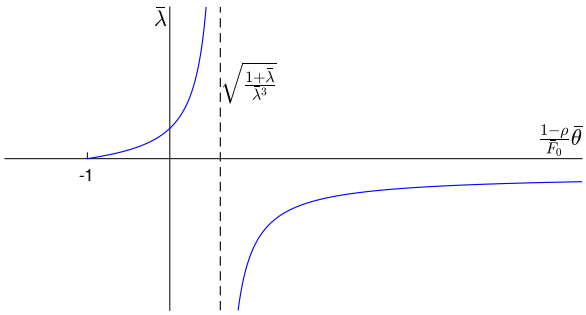

Figure 2: $\bar{\lambda}$ as a function of $\bar{\theta}$ and $\bar{F}_0$.

Steady State Solutions for $\bar{\theta}$

At equilibrium, $h = H(\bar{\theta})$ and $v = V(\bar{\theta}) > 0$. For fixed fluid flow rate, equations (1) and (2) show that $V = 1 = H$ and

$$\frac{1-\rho}{F_0^2}\bar{\theta} = -\frac{1}{H^3} + \frac{1}{1+\lambda} + \frac{\lambda}{(1+\lambda)H} \equiv F(H), \qquad (4)$$

which has a saddle-node bifurcation at $\bar{\theta} = \bar{\theta}_{SN}$, where

$$\bar{\theta}_{SN} \equiv \frac{F_0^2}{(1-\rho)(1+\lambda)}\left(1+\sqrt{\frac{4\lambda^3}{27(1+\lambda)}}\right). \qquad (5)$$

A typical graph is shown in Figure 1. A unique equilibrium solution exists for $\bar{\theta} < F_0^2/(1-\rho)(1+\lambda)$, there are two equilibrium solutions for $F_0^2/(1-\rho)(1+\lambda) < \bar{\theta} < \bar{\theta}_{SN}$, $H = H_-$ and $H = H_+ > H_-$, and no equilibrium solution exists for $\bar{\theta} > \bar{\theta}_{SN}$.

For $\bar{\theta} < \bar{\theta}_{SN}$, we are able to non-dimensionalize the governing equations using the smaller of the two equilibrium solutions and find that the governing equations are then reduced to those studied by Needham *et al.* [13], namely equations (1) and (2) with $\bar{\theta} = 0$, but with λ and F_0 replaced, respectively, by

$$\bar{\lambda} = \frac{H_-^2\lambda}{1+\lambda-H_-^2\lambda}, \qquad \bar{F}_0 = F_0 H_-^{-3/2}, \qquad (6)$$

where $\bar{\lambda} \geq 0$ or $\bar{\lambda} < -3/2$. Figure 2 shows $\bar{\lambda}$ as a function of $\bar{\theta}$ in a typical case. The angle which splits the two regions of $\bar{\lambda}$ is given by

$$\bar{\theta} = \sqrt{\frac{1+\bar{\lambda}}{\bar{\lambda}^3}}\frac{\bar{F}_0^2}{1-\rho} \equiv \bar{\theta}_c. \qquad (7)$$

For $\bar{\theta} < \bar{\theta}_{SN}$, the stability analysis of the steady state solution proceeds in exactly the same manner as detailed by Needham *et al.* [13] and comes to the same result, regardless of the sign of $\bar{\lambda}$. The steady state solution with the smaller thickness, $h = H_-$, loses stability at a larger Froude number (and hence flowrate) than the solution with larger thickness and the range of Froude numbers for which $h = H_+$ is stable is very small [5].

Solutions with constant $\bar{\theta} < \bar{\theta}_{SN}$

We will now simulate the flow through the channel using some small random noise at the inlet and using the scaled system of equations with $\bar{\theta} = 0$, $\lambda = \bar{\lambda}$ and $F_0 = \bar{F}_0$, given by equation (6), with $\bar{\lambda} > 0$ or $\bar{\lambda} < -3/2$. In order to do this, we will use the finite-difference method derived by Kurganov & Tadmor [9] combined with a second-order Runge–Kutta method. By using more precise information on the local propagation speeds, Kurganov & Tadmor [9] have derived a second order accurate scheme that does not rely on the characteristics of the problem other than the local wave speeds. It does not generate spurious oscillations, has a much smaller numerical viscosity compared with other similar schemes and, of particular importance in our work, is able to capture shocks.

When $\bar{\lambda} > 0$ we find that, as expected, lower values of $\bar{\lambda}$ and larger values of $\bar{F}_0$ increase the size of the solutions, as shown in Figure 3. In these simulations, the faster moving roll waves catch and absorb the slower ones and begin to grow. However, due to a lack of a top of the channel, they are unable to maintain their size and revert back to smaller roll waves. For the $\bar{\theta} = 0$ case, as studied by [13], a smaller $\bar{\lambda}$ is equivalent to less damping in the system and so would result in larger roll waves, as we have found. If we consider λ to be constant and consider changes to $\bar{\lambda}$ to be due to changing the value of $\bar{\theta}$, then a smaller $\bar{\lambda}$ is a result of a smaller value of $\bar{\theta}$. As a result of this, the liquid velocity will be higher due to the effects of gravity and hence results in larger roll waves.

For $\bar{\lambda} < -3/2$ we again find that larger values of $\bar{F}_0$ increase the size of the solutions, however lower values of $\bar{\lambda}$ decrease the size of the solutions, as shown in Figure 4. This is due to the waves now propagating backwards relative to the flow, therefore a larger value of $\bar{\lambda}$ (and so larger value of $\bar{\theta}$) results in a more negative propagation speed and hence larger solutions.

From Figures 4a and 4c we can see that for $\bar{\lambda} < -3/2$ we are able to find roll waves that are significantly larger than the average roll wave in the channel. The larger roll waves begin as average roll waves, however they propagate slightly slower than the roll waves around them. When a roll wave behind catches up to them they absorb it which increases their size. This process is then repeated by the larger roll waves, growing in size as they move down the channel as more roll waves catch up with them and are absorbed. Hence, in general, the larger roll waves further down the channel will be bigger than those closer to the inlet. This process is shown in Figure 5 where the roll wave of interest is shown in red. We can see in Figure 5a a roll wave catching up with the roll wave in front of it. Figure 5b then shows it absorbing the faster moving roll wave, after which, as shown in Figure 5c, it has formed into a larger roll wave.

If $\bar{\lambda} < -3/2$ is big enough, these larger roll waves will continue growing until their propagation speed becomes negative relative to the channel, as shown in Figure 6. We will refer to these very large waves as "slug-like". In Figure 6a we can see a larger roll wave at $x \approx 80$, as it grows its propagation speed decreases until it has become slug-like and propagates right–to–left relative to the channel, as shown in Figure 6b. As it propagates negatively it quickly grows larger and accelerates towards the inlet until it reaches the inlet, at which point it is trapped due to imposed inlet conditions, and continues to grow. Since we have made the thin layer approximation, the effect of the upper wall of the channel is neglected, and the wave can grow indefinitely. However, we would expect this process to indicate the formation of a genuine slug if the effects of a channel top were included.

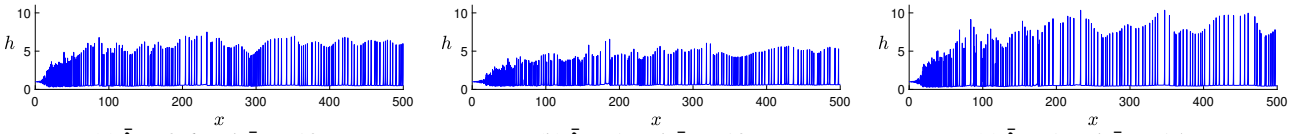

(a) $\bar{\lambda} = 0.6$ and $\bar{F}_0 = 10$. (b) $\bar{\lambda} = 1$ and $\bar{F}_0 = 10$. (c) $\bar{\lambda} = 1$ and $\bar{F}_0 = 15$.

Figure 3: The solutions at $t = 1000$ for $R_l = 50$ and $\rho = 0.1$ and varying $\bar{\lambda} > 0$ and $\bar{F}_0$.

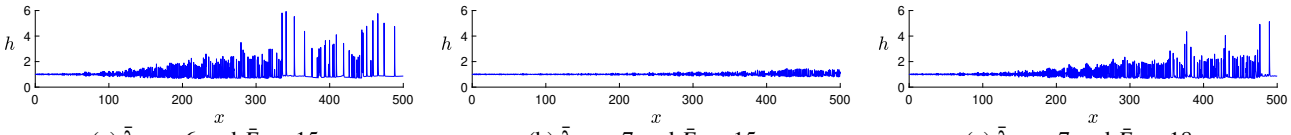

(a) $\bar{\lambda} = -6$ and $\bar{F}_0 = 15$. (b) $\bar{\lambda} = -7$ and $\bar{F}_0 = 15$. (c) $\bar{\lambda} = -7$ and $\bar{F}_0 = 18$.

Figure 4: The solutions at $t = 1000$ for $R_l = 50$ and $\rho = 0.1$ and varying $\bar{\lambda} < -3/2$ and $\bar{F}_0$.

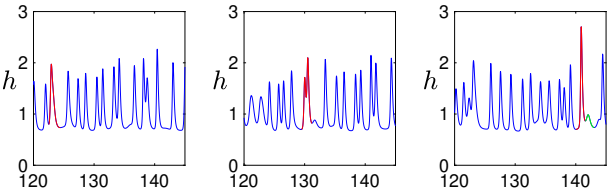

(a) $t = 701$. (b) $t = 710$. (c) $t = 723$.

Figure 5: The solutions as a larger roll wave is formed for $\bar{\lambda} = -5$, $R_l = 50$, $\rho = 0.1$ and $\bar{F}_0 = 12$.

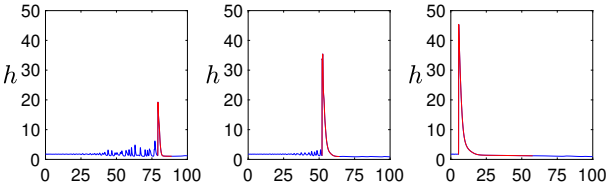

(a) $t = 250$. (b) $t = 300$. (c) $t = 350$.

Figure 6: The solutions for $\bar{\lambda} = -2.85$, $\bar{F}_0 = 6.45$, $R_l = 50$ and $\rho = 0.1$.

Solutions with sinusoidally-varying $\bar{\theta}$

In order to solve the IVP for a non-constant $\bar{\theta}$ we use equations (1) and (2) and define a function for $\bar{\theta}$. We will begin by letting

$$\bar{\theta} = K \frac{F_0^2}{1-\rho} \sin\left(\frac{2\pi x}{L} a + b\pi\right), \tag{8}$$

where a is the number of undulations, b can be set to choose whether we start by going uphill or downhill and K controls the maximum size of $\bar{\theta}$.

By varying the parameters we find, as we found previously, by increasing F_0 or making $\bar{\theta}$ more negative we produce larger roll waves. When investigating $0 < \bar{\theta} < \bar{\theta}_c$ we find that increasing $\bar{\theta}$ decreases the size of the roll waves. However, when $\bar{\theta}$ is increased enough, such that $\bar{\theta} > \bar{\theta}_c$, we begin to see the roll waves absorbing each other, as in the previous section for $\bar{\lambda} < -3/2$, and increasing $\bar{\theta}$ increases the size of these roll waves until we get slug-like waves forming, as shown in Figure 7 where, from equation (5), $\theta = \theta_{SN}$ occurs when $K \approx 0.636$.

By comparing Figures 7c and 7e we see that for $\bar{\theta} > \bar{\theta}_c$ if F_0 is large enough slug-like waves form. Further, we can see from Figures 7d and 7f that when $\bar{\theta} > \bar{\theta}_{SN}$ we always get slug-like waves forming. When these slug-like waves form they begin propagating back towards the inlet, however as the slope lessens their propagation speed tends to zero and they reach a point of equilibrium maintaining their position in the pipe, slowly growing as roll waves reach them and are absorbed.

Figure 8 shows the effects of varying a and b for $F_0 = 10$, $K = 0.4$, $\bar{\lambda} = 1$, $R_l = 50$ and $\rho = 0.1$. We can see that as the channel goes uphill the roll waves decrease in size to a point where the flow has become stratified flow with a disturbance and as the flow goes downhill the roll waves significantly increase in size. We may also observe that the liquid builds up in the uphill regions, as shown in Figure 8c for $0 < x < 150$ for which the liquid is highest for $60 < x < 65$ which corresponds to the largest value of $\bar{\theta}$. As a result of this we can see in Figure 8 that we produce larger roll waves in a downhill region when it comes after an uphill region.

In Figures 8e and 8f we have set $\bar{\theta} = 0$ in the second half of the channel in order to study the effects of having a channel which goes either uphill or downhill before levelling into a flat region. We can see that for $b = 0$, where we have an uphill region before the flat region, we have produced larger roll waves with greater separation. By comparing these solutions with those found in a horizonatal channel [6] we find that the horizontal channel solutions fall between the two shown here. Hence, although uphill inclinations have a dampening effect on the flow, the liquid build-up that occurs causes an amplifying effect on the size of the roll waves when the inclination angle decreases. This is of particular importance as subsea natural gas pipelines must travel uphill as they leave the sea before travelling across land.

Conclusions

In this paper we extended the work of Giddings & Billingham [5] to further investigate the effects of inclination on the development of a slug flow regime. For a channel with constant inclination to the horizontal, we found that a saddle-node bifurcation means that no spatially-uniform steady state solution exists for sufficiently uphill flows, in line with similar observations in models for laminar stratified flows [16]. When we considered noise-driven flows in a channel with a sinusoidally-varying inclination, we found that, at points in the channel where the inclination equals the saddle-node bifurcation angle, the thickness of the liquid layer grows locally, leading to a slug-like structure that we hypothesise indicates the initiation of a slug in the full model. Finally, we considered the effects of having a channel with either uphill or downhill inclination before levelling into a flat region. This leads to the discovery that an uphill section followed by a horizontal section produces larger roll waves in the horizontal section than would otherwise be formed.

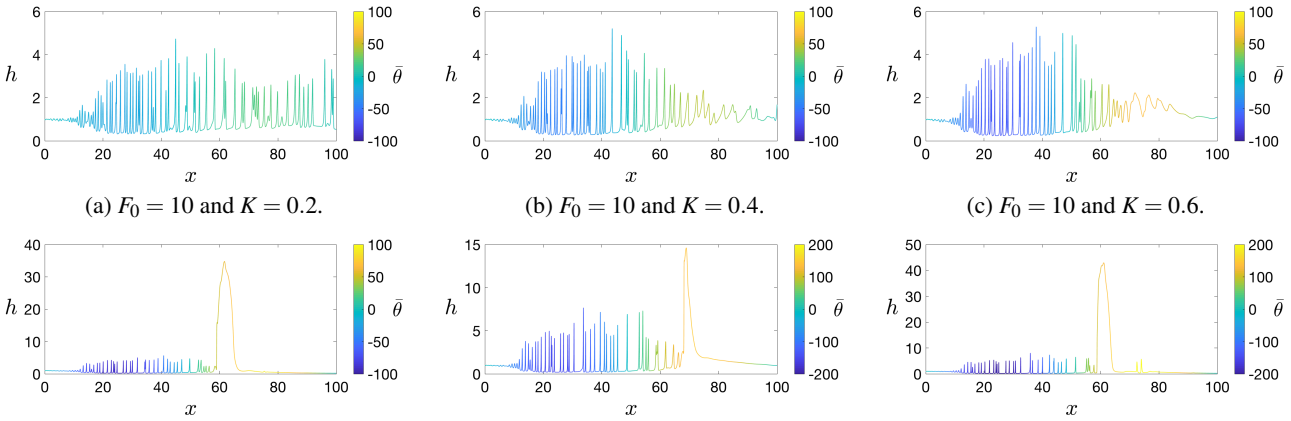

(a) $F_0 = 10$ and $K = 0.2$. (b) $F_0 = 10$ and $K = 0.4$. (c) $F_0 = 10$ and $K = 0.6$.

(d) $F_0 = 10$ and $K = 0.8$. (e) $F_0 = 15$ and $K = 0.6$. (f) $F_0 = 15$ and $K = 0.8$.

Figure 7: The effects of varying K and F_0 for $\lambda = 1$, $R_l = 50$, $\rho = 0.1$, $a = 1$ and $b = 1$.

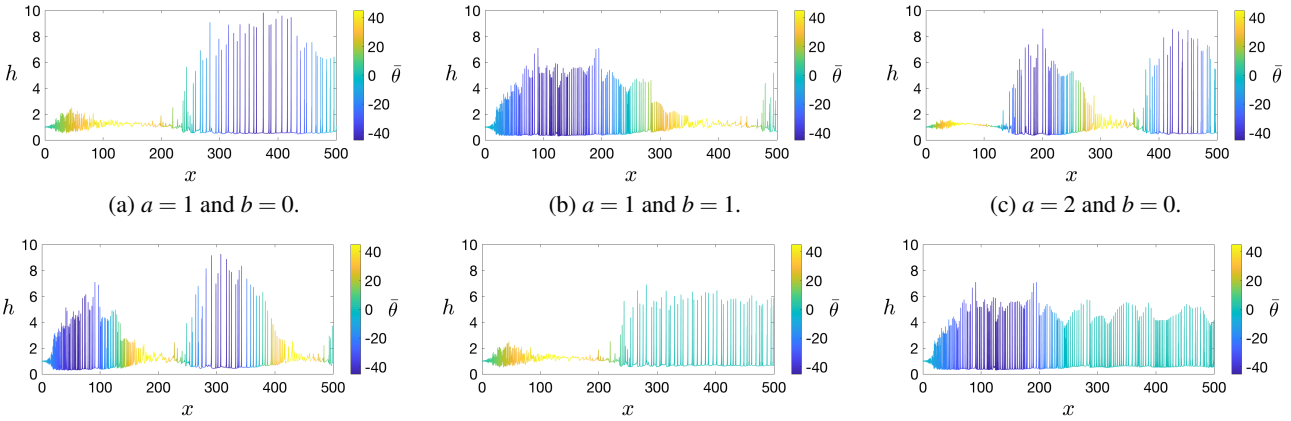

(a) $a = 1$ and $b = 0$. (b) $a = 1$ and $b = 1$. (c) $a = 2$ and $b = 0$.

(d) $a = 2$ and $b = 1$. (e) $b = 0$ with a flat channel end. (f) $b = 1$ with a flat channel end.

Figure 8: The effects of varying a and b for $F_0 = 10$, $K = 0.4$, $\lambda = 1$, $R_l = 50$ and $\rho = 0.1$.

References

[1] Andritsos, N. and Hanratty, T. J., Interfacial instabilities for horizontal gas-liquid flows in pipelines, *Int. J. Multiph. Flow*, **13**, 1987, 583–603.

[2] Balmforth, N. J. and Mandre, S., Dynamics of roll waves, *J. Fluid Mech.*, **514**, 2004, 1–33.

[3] Funada, T. and Joseph, D. D., Viscous potential flow analysis of Kelvin-Helmholtz instability in a channel., *J. Fluid Mech.*, **445**, 2001, 263–283.

[4] Giddings, J. A., *One Dimensional Models for Slugging in Channel Flow*, Ph.D. thesis, School of Mathematical Sciences, The University of Nottingham, UK, 2017.

[5] Giddings, J. A. and Billingham, J., The effect of inclination on the development of slugging in channel flow, *Submitted to IMA J. Appl. Math.*.

[6] Giddings, J. A., Billingham, J. and Cox, S. M., One dimensional models for slugging in horizontal channel flow, *In Progress*.

[7] Johnson, G. W., Bertelsen, A. F. and Nossen, J., A mechanistic model for roll waves for two-phase pipe flow, *AIChE Journal*, **55**, 2009, 2788–2795.

[8] Kranenburg, C., On the evolution of roll waves, *J. Fluid Mech.*, **245**, 1992, 249–261.

[9] Kurganov, A. and Tadmor, E., New high-resolution central schemes for nonlinear conservation laws and convection–diffusion equations, *J. Comput. Phys.*, **160**, 2000, 241–282.

[10] Lin, P. Y. and Hanratty, T. J., Prediction of the initiation of slugs with linear stability theory., *Int. J. Multiph. Flow*, **12**, 1986, 79–98.

[11] Mata, C., Pereyra, E., Trallero, J. L. and Joseph, D. D., Stability of stratified gas–liquid flows., *Int. J. Multiph. Flow*, **28**, 2002, 1249–1268.

[12] Montes, S., *Hydraulics of open channel flow*, ASCE, 1998.

[13] Needham, D. J., Billingham, J., Schulkes, R. M. S. M. and King, A. C., The development of slugging in two-layer hydraulic flows, *IMA J. Appl. Math.*, **73**, 2008, 274–322.

[14] Rouse, H., *Fluid mechanics for hydraulic engineers*, Dover Publications Inc., 1938.

[15] Taitel, Y. and Dukler, A. E., A model for predicting flow regime transitions in horizontal and near horizontal gas–liquid flow., *AIChE Journal*, **22**, 1976, 47–55.

[16] Thibault, D., Munoz, J.-M. and Liné, A., Multiple holdup solutions in laminar stratified flow in inclined channels, *Int. J. Multiph. Flow*, **73**, 2015, 275–288.